

Observation of the Direct and Sequential Breakup of ${}^7\text{Li}$ from ${}^{12}\text{C}$ and ${}^{208}\text{Pb}$ Targets at 70 MeV

A. C. Shotter,^(a) A. N. Bice, J. M. Wouters, W. D. Rae, and Joseph Cerny

Lawrence Berkeley Laboratory and Department of Chemistry, University of California, Berkeley, California 94720
(Received 14 October 1980)

A study has been made of the breakup of 70-MeV ${}^7\text{Li}$ into the $\alpha + t$ channel. For reactions on a ${}^{12}\text{C}$ target the ${}^7\text{Li}$ breakup proceeds sequentially through its 4.63-MeV, ${}^7_2^-$ state. For reactions on a ${}^{208}\text{Pb}$ target, there is evidence both for sequential breakup and for an additional breakup process which does not proceed through an excited state of ${}^7\text{Li}$. This latter process is attributed to direct projectile breakup in the nuclear field of the target.

PACS numbers: 25.70.-z

The subject of projectile dissociation in the field of a target nucleus encompasses a variety of phenomena and is currently attracting substantial interest.¹⁻⁵ For projectile energies below the Coulomb barrier, the projectile may be excited by the electromagnetic field between the incident channel nuclei. If the excited states are above the threshold for particle emission, and have small energy widths, the projectile will in most instances sequentially breakup beyond the influence of the target's nuclear field.⁶ In contrast, at high energies (~ 100 MeV/A) a projectile incident on the peripheral region of the target nucleus might be expected to undergo a rapid fragmentation in the surface field of the nucleus.⁷

For a projectile with an intermediate energy it should be possible to identify a transition from sequential breakup to a rapid nonsequential process, i.e., a direct breakup mode. A recent study⁸ of the breakup of 75-MeV ${}^6\text{Li}$ projectiles into $\alpha + d$ fragments has revealed evidence for two possible mechanisms. The first was identified as sequential breakup through the 2.18-MeV ${}^6\text{Li}$ state, while the second could not be correlated with transitions through any specific state. However, this lack of correlation could also have been due to transitions through the higher ${}^6\text{Li}$ states which all have large energy widths. For the observation of a possible direct projectile breakup a projectile should be used with a large energy separation between the breakup threshold and the next excited state. A suitable projectile is ${}^7\text{Li}$, in which the first α decaying state is at 4.63 MeV, 2.16 MeV above the $\alpha + t$ breakup threshold. By an appropriate choice of detector geometry, direct ${}^7\text{Li}$ breakup events with an $\alpha + t$ relative energy smaller than ~ 2.1 MeV can be clearly distinguished from all possible sequential-breakup events.

We present here results of an investigation of

70-MeV ${}^7\text{Li} \rightarrow \alpha + t$ breakup on ${}^{12}\text{C}$ and ${}^{208}\text{Pb}$ targets. For those breakup events in which the relative energy between the fragments is below 3 MeV, it is found that the breakup of ${}^7\text{Li}$ on the ${}^{12}\text{C}$ target is predominantly sequential—proceeding through the 4.63-MeV state of ${}^7\text{Li}$. In contrast, the breakup of ${}^7\text{Li}$ on the ${}^{208}\text{Pb}$ target has two components, this sequential component involving excitation to the 4.63-MeV state as well as a direct component.

The experiment was performed with use of a 70-MeV ${}^7\text{Li}$ beam produced by the Lawrence Berkeley Laboratory 88-in. cyclotron. The breakup fragments from the decay of ${}^7\text{Li}^*$ are confined to a cone of angular width that is determined by their relative energy ϵ , and the laboratory energy of the ${}^7\text{Li}^*$. For the detection of those events in which ϵ is small, it is essential to have the fragment detectors in close proximity. This was achieved by constructing two particle telescopes in close vertical geometry, with one telescope above and the other below the reaction plane. The telescopes consisted of pairs of ΔE (200 μm) and E (5 mm) detectors manufactured on the same silicon wafer such that the vertical angular acceptance of the telescopes was 1.5° to 9.9° and the horizontal angular acceptance was 3° . Reject detectors placed behind the E detectors were employed to veto high-energy events.

Figure 1(a) presents coincidence data for the ${}^7\text{Li} + {}^{12}\text{C}$ reaction at 15° in the laboratory, in which the summed energy of coincident events in the two telescopes is displayed, with the requirement that an α particle be recorded in one and a triton in the other. The three peaks correspond to those breakup events which leave the ${}^{12}\text{C}$ target in the ground state or excited to the 4.4-MeV, 2^+ or 9.6-MeV, 3^- states. The angular distribution of the production of ${}^7\text{Li}^*$ (4.63 MeV) for the ${}^{12}\text{C}$ remaining in the ground state is shown in Fig.

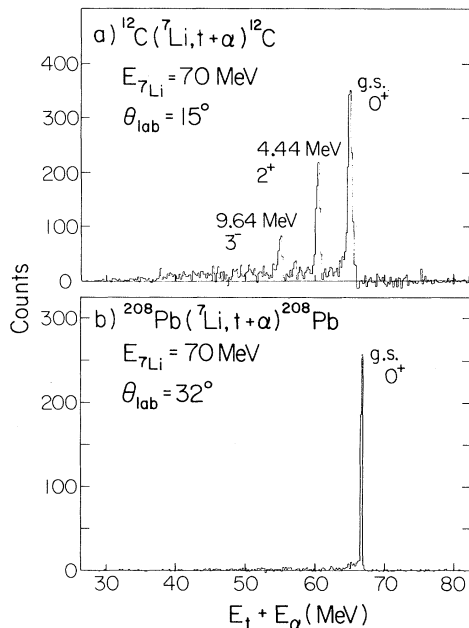


FIG. 1. (a) Summed energy spectrum for coincident $\alpha + t$ particles from the breakup of ${}^7\text{Li}$ on ${}^{12}\text{C}$ target nuclei. (b) As for (a), but for a ${}^{208}\text{Pb}$ target.

2(a). (The angular distribution has been corrected for the α detection efficiency. This efficiency was determined by a Monte Carlo simulation technique that assumed an isotropic distribution of the α - t fragments in the ${}^7\text{Li}^*$ center-of-mass system and a decay energy of $\epsilon = 2.16$ MeV.)

Further interpretation of the character of these breakup events can be obtained from the α or t projected energy spectra for coincident $\alpha + t$ events that yield a total energy corresponding to one of the peak energies in Fig. 1(a). Such a projected spectrum for the t corresponding to the ${}^{12}\text{C}$ ground-state transition is shown in Fig. 3(a). The two peaks of Fig. 3(a) correspond to the two kinematically allowed t energies from the breakup of ${}^7\text{Li}^*$ (4.63 MeV). The shape of these peaks is determined by the geometry of the two telescopes as well as by the center-of-mass breakup energy, ϵ , and the energy of the recoiling ${}^7\text{Li}^*$ projectile. Calculated energy windows in this projected spectrum for breakup from the 4.63-MeV state ($\epsilon = 2.16$ MeV) are indicated in Fig. 3(a) by arrows. It is seen that most of the events are located within these narrow limits.

If direct breakup had occurred in the field of the target nucleus the relative energy, ϵ , between the α and t would no longer be restricted to a definite value corresponding to the decay of

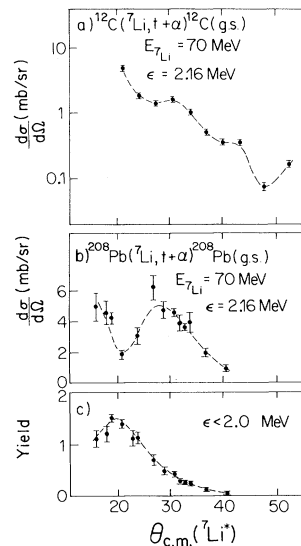


FIG. 2. (a) The differential cross section for the $\alpha + t$ breakup of 70-MeV ${}^7\text{Li}$ from the ground state of ${}^{12}\text{C}$. [The dashed lines in (a), (b), and (c) are to guide the eye.] (b) The differential cross section for the sequential $\alpha + t$ breakup of 70-MeV ${}^7\text{Li}$ from the ground state of ${}^{208}\text{Pb}$, following excitation to the 4.63-MeV state of ${}^7\text{Li}$. (c) The yield of direct-breakup events as a function of ${}^7\text{Li}^*$ c.m. angle for ${}^7\text{Li}$ scattering from the ${}^{208}\text{Pb}$ target.

an excited state of ${}^7\text{Li}$, but rather the value of ϵ could vary over some continuous distribution related to the momentum distribution of the fragments in the projectile ground state.⁹ From Fig. 3(a) there is little, or no, evidence of such a distribution of ϵ , since the projected spectrum is consistent with a single value of $\epsilon = 2.16$ MeV arising from the decay of the 4.63-MeV state of ${}^7\text{Li}$. In fact, for all detector angles between 13° and 33° the shapes of the projected spectra for the ${}^{12}\text{C}$ ground-state transition are similar.

The corresponding experimental results for the ${}^{208}\text{Pb}$ target are shown in Figs. 1(b), 2(b), 2(c), 3(b), and 3(c). The summed energy of coincident $\alpha + t$ events is shown in Fig. 1(b), in which it is seen that the majority of breakup events into the $\alpha + t$ channel leave the target in its ground state. The projected energy spectrum for the t fragment corresponding to this transition, and for the detector system set at 32° in the laboratory, is shown in Fig. 3(b); arrows indicate the triton energy limits for a sequential breakup of ${}^7\text{Li}^*$ (4.63 MeV). A projected energy spectrum of the t fragment when the detectors are located at 18° is shown in Fig. 3(c) [the arrows have the same significance as in Fig. 3(b)].

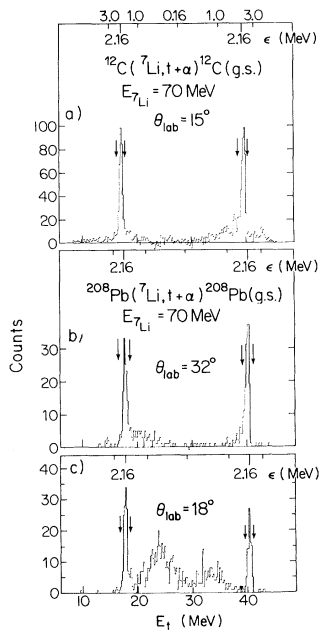


FIG. 3. (a) The triton energy spectrum for coincident $\alpha + t$ events in which the residual ^{12}C nucleus remained in its ground state. The detector system was located at $\theta_{\text{lab}} = 15^\circ$. (b) The triton energy spectrum for coincident $\alpha + t$ events in which the residual ^{208}Pb nucleus remained in its ground state. The detector system was located at $\theta_{\text{lab}} = 32^\circ$. (c) As for (b), but with the detector system at $\theta_{\text{lab}} = 18^\circ$.

It is apparent that Figs. 3(a) and 3(b) are similar, showing little evidence for direct breakup. In contrast, data taken on ^{208}Pb at the more forward angles, presented in Fig. 3(c), include events with a continuous distribution of ϵ which cannot arise from discrete states of ${}^7\text{Li}$. This is taken as evidence of direct breakup.

The angular distribution of the sequential component involving excitation of the 4.63 MeV ($\epsilon = 2.16 \text{ MeV}$) state is shown in Fig. 2(b). This angular distribution is corrected for the change of $\alpha + t$ detection efficiency as a function of angle. The yield of the direct component corresponding to $\epsilon \leq 2.0 \text{ MeV}$ is shown in Fig. 2(c), but is not corrected for detection efficiency changes since this would require specific assumptions to be made about the momentum distribution of the α and t in the ${}^7\text{Li}^*$ center-of-mass system.

The events occurring with $\epsilon \leq 2.0 \text{ MeV}$ have been attributed to a direct breakup of ${}^7\text{Li}$. Such events might be thought of as arising (a) by a rapid reemission of a transferred projectile fragment and/or (b) by inelastic scattering of the projectile to the continuum of the $\alpha + t$ system. For

process (a), the fragment reemission would have to occur within the nuclear transit time; otherwise the momentum correlation between the α and t fragments would be lost. The distribution of relative energies between the fragments for a direct-breakup process is determined by the phase space of the final-state particles, by their mutual Coulomb interaction, and by their momentum distribution in the bound ${}^7\text{Li}$ system. Since the outgoing fragments have different Z/A ratios, the target-fragment Coulomb interaction will distort the initial momentum distribution.¹⁰ In Fig. 3(c) it can be seen that the yield of tritons with lower laboratory energies is enhanced. This asymmetry is observed at all angles measured and may be due to this Coulomb distortion.

There is a distinct difference between the angular distribution for the direct component $\epsilon \leq 2.0 \text{ MeV}$, and the sequential component $\epsilon = 2.16 \text{ MeV}$. It is possible to speculate that the direct component originates from a greater overlap between the incident nuclei than that needed for simple projectile excitation, which might result in a nuclear deflection to smaller angles than the grazing angle of $\sim 30^\circ$. One could also argue that both the direct- and sequential-breakup processes have enhanced yield at forward angles due to strong Coulomb effects. However, an investigation of the breakup of 32-MeV ${}^7\text{Li}$ projectiles from ^{197}Au gave a very small cross section for Coulomb breakup.¹¹

Whatever the precise reaction mechanisms are, it will be of great interest to determine how the direct- and sequential-breakup components vary with incident energy, especially in the region 10–100 MeV/A, since this could lead to a much greater understanding of fragmentation processes in general.

This work was supported by the Nuclear Physics and Nuclear Sciences Division of the U. S. Department of Energy under Contract No. W-7405-ENG-48.

^(a)Permanent address: Physics Department, University of Edinburgh, Edinburgh EH9 3JZ, Scotland.

¹D. K. Scott, in Proceedings of the International Conference on Nuclear Physics, Berkeley, California, August 1980 (to be published).

²G. Baur, R. Shyam, F. Rösler, and D. Trautmann, Phys. Rev. C **21**, 2668 (1980).

³J. R. Wu, C. C. Chang, and H. D. Holmgren, Phys. Rev. Lett. **40**, 1013 (1978).

⁴K. W. McVoy and M. C. Nemes, Z. Phys. A **295**, 177

(1980).

⁵C. K. Gelbke, M. Bini, C. Olmer, D. L. Hendrie, J. L. Laville, J. Mahoney, M. C. Mermaz, D. K. Scott, and H. H. Wieman, *Phys. Lett.* **71B**, 83 (1977).

⁶H. W. Wittern, *Phys. Lett.* **32B**, 441 (1970).

⁷A. S. Goldhaber and H. H. Heckman, *Annu. Rev. Nucl. Sci.* **28**, 161 (1978).

⁸C. M. Castaneda, H. A. Smith, P. P. Singh, and

H. Karwowski, *Phys. Rev. C* **21**, 179 (1980).

⁹R. Shyam, G. Baur, F. Rösler, and D. Trautmann, *Phys. Rev. C* **19**, 1246 (1979).

¹⁰A. Gamp, J. C. Jacmart, N. Poffe, H. Doubre, and J. C. Roynette, *Phys. Lett.* **74B**, 215 (1978).

¹¹J. L. Quebert, B. Frois, L. Marquez, G. Sousbie, R. Ost, K. Bethge, and G. Gruber, *Phys. Rev. Lett.* **32**, 1136 (1974).

Nuclear-Shape Effects in the Inelastic Scattering of Polarized Deuterons at 56 MeV

K. Hatanaka

Research Center for Nuclear Physics, Osaka University, Suita, Osaka 565, Japan

and

M. Nakamura, K. Imai, T. Noro, H. Shimizu, H. Sakamoto, J. Shirai,
T. Matsusue, and K. Nisimura

Department of Physics, Kyoto University, Kyoto 606, Japan

(Received 22 September 1980)

Differential cross sections and vector analyzing powers for the deuteron elastic and inelastic scattering from ^{24}Mg and ^{28}Si have been measured at 56 MeV. The coupled-channels analysis has been performed to obtain the simultaneous fits to the elastic- and inelastic-scattering data. The dependence of the coupled-channels calculations on the shape of nuclei has been investigated in comparison with the proton inelastic scattering.

PACS numbers: 25.50.Dt, 21.10.Ft, 24.70.+s

In recent years, there have been many studies for the determination of the shape of nuclei. It has been pointed out that the coupled-channels (CC) analysis of the elastic and inelastic scattering of polarized protons or deuterons is sensitive to the shape of nuclear deformation.¹⁻⁵ For a $0^+ - 2^+$ rotational excitation, for example, there are two nuclear matrix elements: one between 0^+ and 2^+ ; another between two 2^+ functions. They are related to the $E2$ transition probability and quadrupole moments of the excited state, respectively. The sign of the quadrupole moment is related to the sign of the nuclear matrix element and will affect the results of the calculation.⁶ A coupled-channels analysis of the proton inelastic scattering at 65 MeV was recently performed and it was found that the diffraction pattern of the angular dependence of the asymmetry showed shifts in different directions whether prolate or oblate static deformation was present.⁷ The larger shifts were reported for the vector analyzing power of the deuteron elastic and inelastic scattering around 10 MeV.⁸ Although the strong dependence of the deuteron scattering on the nuclear deformation has been suggested by some authors,^{9,10} the experiments were concentrated at low energies.

It is interesting to investigate this problem at higher energies where the reaction mechanism is considered to be direct and almost free from the compound nucleus effects. In this Letter we report the measurements and CC analysis of the deuteron inelastic scattering to the first 2^+ states of ^{24}Mg and ^{28}Si at 56 MeV.

The experiments were performed with 56 MeV vector polarized deuterons from the AVF cyclotron at the Research Center for Nuclear Physics, Osaka University. Polarized deuterons were produced by the atomic-beam-type ion source.¹¹ The beam current was 5–20 nA on target. The beam polarization was monitored continuously during the measurements by a ^{12}C polarimeter and was (70–80)% of the ideal value. The sign of the beam polarization was changed every second. The scattered deuterons were detected by a pair of counter telescopes placed at symmetric angles to the beam direction. Each telescope consisted of a 400- μm -thick transmission-type Si detector and a 15-mm-thick high-purity Ge detector cooled by liquid nitrogen. The particle identification was made with ΔE and E signals. The enriched ^{24}Mg and natural ^{28}Si targets were self-supporting metallic foils with thickness of about 3 mg/cm².